Induction Thermography as a Tool for Reliable Detection of Surface Defects in Forged Components

Udo NETZELMANN and Günter WALLE,
Fraunhofer Institute for Nondestructive Testing
Campus, Bldg. E 3 1
66123 Saarbrücken, Germany
Tel: +49 681 9302 3873, Fax: +49 681 9302 5901
E-mail: udo.netzelmann@izfp.fraunhofer.de

Abstract

Dynamic thermography with inductive excitation is analysed as an alternative to magnetic particle inspection or to eddy current testing. Given by the relation of the electromagnetic skin depth, the thermal penetration depth and the crack dimensions to be detected, different regimes for defect detection are identified. The effect of the crack parameters length, depth and inclination angle are discussed. In ferritic steel, at induction frequencies of 100-200 kHz, perpendicular open cracks with a length of 7.5 mm were detectable when their depth was minimum 0.15 mm. For inclined cracks, the sensitivity is even higher. Experiments were performed on cold and warm forged steel components. The signal-to noise ratio obtained from defects was usually high, the critical limitation on technical surfaces is the background due to surface roughness and due to surface contamination. A series investigation on forged components showed a good probability of detection and a low false alarm rate compared to magnetic particle testing. The short testing times of a few 100 ms per object view will allow short cycle times for mass products.

Keywords: forging, skin depth, thermal diffusion, thermography, induction, false alarm rate

1. Introduction

There are high requirements for stiffness and toughness of cold and warm forged components. In particular defects close to the surface may influence the stiffness or lead to failure. Testing for these defects is therefore of particular importance. Due to defects in the raw materials and due to disturbations in the process it is not always possible to achieve absence of surface defects. Typical defects are surface cracks visible by eye and microcracks. The forging process sometimes causes initially open cracks to the surface to be closed, making them invisible for visual inspection. Such defects are difficult to detect.

In industrial practice, magnetic particle testing and eddy current testing are employed both for 100%-testing of components and for spot checks. Eddy current is usually applied on components with simple geometry. A major drawback of eddy current testing is that relatively broad macro cracks visible for the eye are often not detected. It is often not possible to detect shallow inclined cracks. Cracks below the surface are hardly detected, and generally the crack depth can not be quantified. In this contribution, induction thermography is featured as an interesting alternative to established testing techniques.

2. Induction Thermography

A high frequency induction coil in the neighbourhood of the test object generates eddy currents in pulses of typically 50-500 ms length (Fig. 1). Crack detection is based on the changes of the distribution of the locally induced eddy currents due to the crack, which lead to locally changed eddy current losses near the cracks. Hence, a higher heat generation occurs near the crack which can be used for thermographic heat detection. Perpendicular cracks, but also slanted cracks can be detected in this way. Typical transient heating is up to about some ten degrees above ambient temperature.

First applications in steel industry were reported more than two decades ago [1], where continuous inductive heating on moving steel bars was applied to detect longitudinal cracks. Further, the technique has been applied using periodic heating and phase sensitive detection for characterization of coating adhesion [2] and using pulsed excitation for crack detection in turbine blades [3]. New applications on steel components and carbon fibre reinforced polymers [4] and analytical and numerical modelling of the signal from cracks were reported [5,6]. The role of the current distributions was enlightened recently [7].

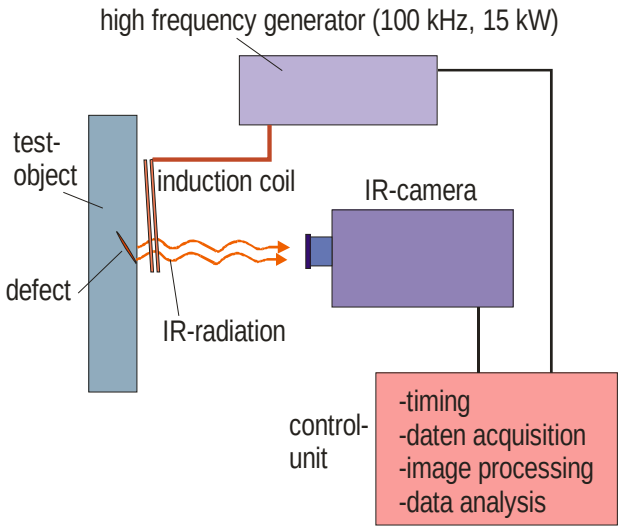

Fig. 1: Scheme of a set-up for induction thermography

3. Material classes and characteristic lengths

In order to the estimate the ability to detect defects in materials by induction thermography, it is important to consider the characteristic lengths like the electrical skin depth δ (defined by the electrical conductivity σ and the magnetic permeability μ) and the thermal penetration length μ_T (sometimes called thermal skin depth) for the material under investigation (Fig. 2).

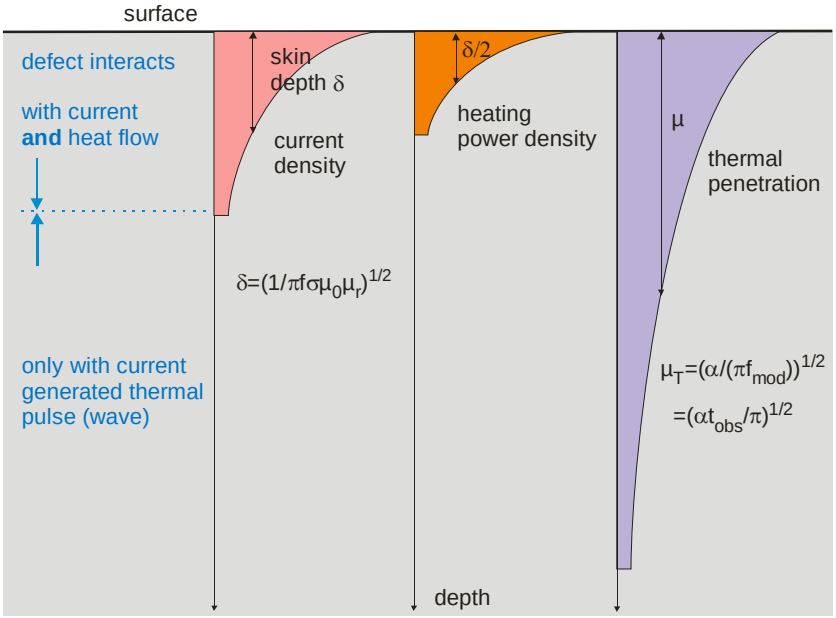

Fig. 2: Characteristic lengths for defect detection

The induction current flow is characterized by the electromagnetic skin depth. According to the Joule heating law the characteristic length for induction heating is half of the skin depth. Thermal penetration is determined by the thermal diffusivity α of the material and by the observation time t_{obs} after pulsed heating or the amplitude modulation with f_{mod} in the lock-in technique.

Table 1 lists some materials and typical values for an induction frequency of 100 kHz and an observation time of 100 ms.

group		electrical conductivity in 10^6 S/m	relative magnetic permeability	thermal diffusivity in 10^{-6} m²/s	electromagnetic skin depth in mm (100 kHz)	thermal penetration depth in mm (t=0.1 s)
I	cast iron	6.2	200	14.9	0.045	2.44
	nickel, pure	14.62	100	22.9	0.042	3.03
II	silver, pure	62.87	1	173	0.201	8.32
	zinc, rolled	16.24	1	41.2	0.395	4.06
	aluminium 2014-T6	22.53	1	73	0.335	5.40
	copper, pure	60.09	1	112	0.205	6.71
III	Inconel 600	0.98	1	3.13	1.608	1.12
	stainless steel 316	1.33	1	7.09	1.380	1.68
	titanium 6AL-4V	0.58	1	6.59	2.090	1.62
IV	carbon fiber reinforced polymer	0.001	1	3.65	50	1.21
	SiC Ceramic	0.00005-0.001	1	0.000022	50-225	2.97

Table 1: Electrical and thermal penetration depths for various materials

Four groups of materials can be identified. Due to their high magnetic permeability, the ferromagnetic metals (group I) have a very small skin depth compared to the thermal penetration. Only a thin surface layer generates the heat. The non-magnetic metals in group II are often good electrical conductors, but their skin depth is still one order below the thermal penetration. In group III one can find metallic alloys with relatively poor electrical and thermal conduction, like Inconel or stainless steel. Here, the electromagnetic and thermal penetration depth are of comparable size for the given parameters. Finally, the materials of group IV like carbon fibre reinforced and semiconducting ceramic materials have an electromagnetic skin depth significantly larger than the thermal penetration.

The interaction with the defect is different for these groups. For the non-magnetic metals (group II and III), the electromagnetic skin depth is often of the order of the typical defect depth to be found (Fig. 3). Blocking of the current lines by the crack and its interaction with the thermal sources in the near-field is dominating the processes leading to an observable temperature contrast. For the magnetic metals, the skin depth often is small compared to the typical depth. Additional heat generating surfaces (the crack flanks) are the main source for the early thermal contrast. The materials of groups I and II have a different appearance of the crack in the thermographic image [8].

An interaction of the heat pulse generated close to the surface with a defect lying below the electromagnetic skin depth is possible and can lead to an observable thermal contrast. This mechanism is not present in eddy current or magnetic particle inspection.

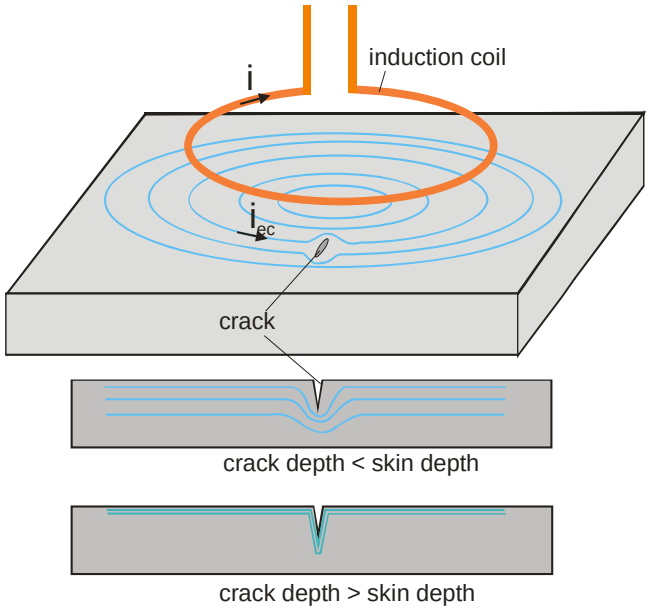

Fig. 3: Scheme of a set-up for induction thermography

Finally, detection of crack-like small defects in the CFRP or electrical conducting ceramics may be difficult, as the heat input is evenly spread.

4. Examples of Application

In Fig. 4, a defect at the surface of a forged piston is shown. The thermographic image represents the thermal radiation by colors or grey values, where blue are lower and red higher temperatures. The defect is appearing as a red line parallel to the crack opening.

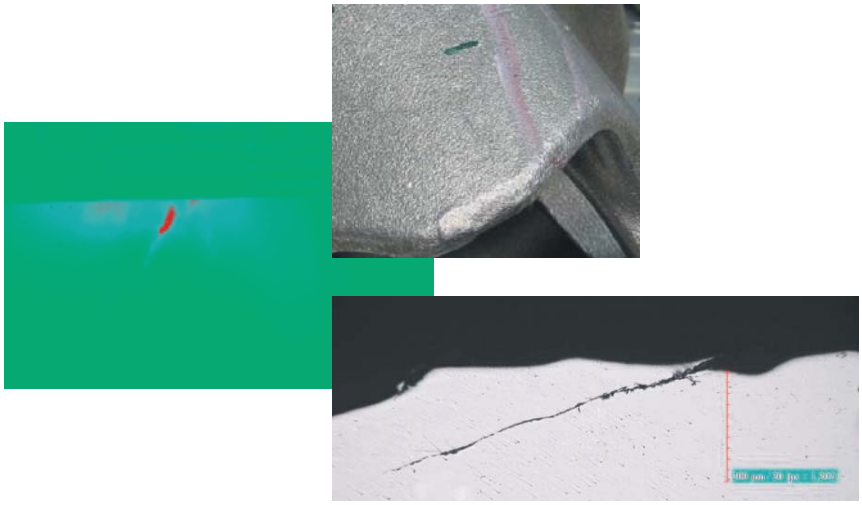

Fig. 4: Thermographic indication of a defect. Upper right: Photo of the defect area, lower right: metallographic cross section

The specimen was later cut at the crack position. The metallographic image shows an inclined crack with a maximum depth (measured perpendicular to the surface) of 200 µm.

In Fig. 5, a spur wheel is shown which has a line of cracks in the hollow. An imaging filter was additionally applied to suppress a disturbing influence of the curvature. In a subsequent metallographic inspection, a crack depth up to 4 mm was found.

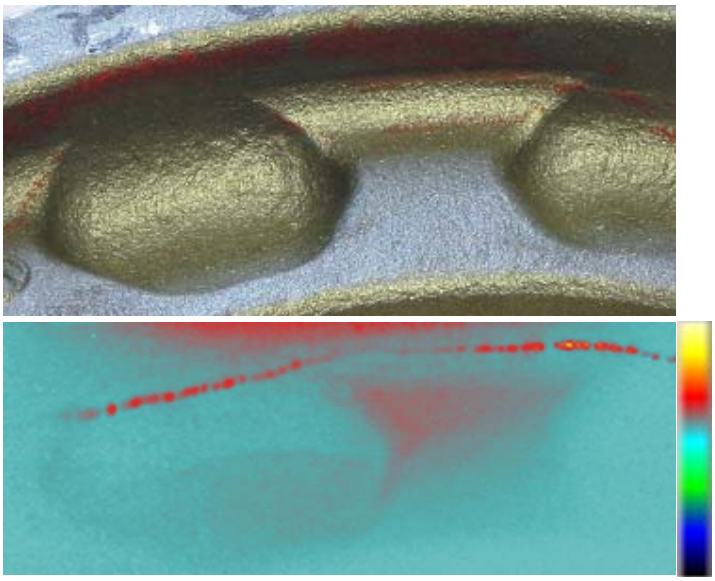

Fig 5: Crack line in the hollow of a spur gear. Top: Photo of the defect area, bottom: thermographc image

Fig. 6 shows another crack indication in a forged component. Here, the thermographic image sequence was processed by a pulse-phase algorithm to obtain a phase image (at 12 Hz) that suppresses inhomogeneous heating and reflected radiation. The crack is represented with a high contrast and can easily be segmented by automated image processing.

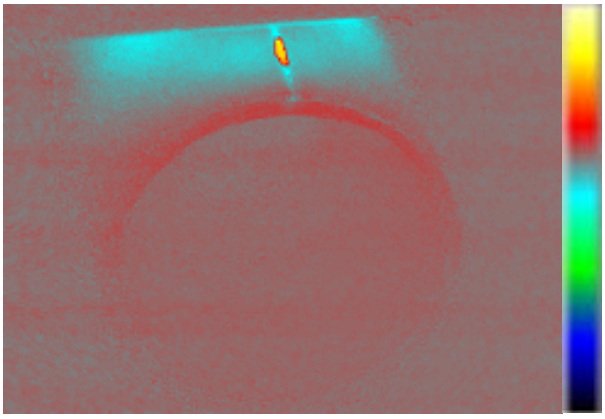

Fig. 6: Crack in a small automotive component

Detection of defects is not limited to outer surfaces, but is also possible in hollow shapes, as long as visibility for the infrared optics is given.

In further experimental and theoretical investigations on ferritic and other materials [6-9], the dependence of the defect signal on crack depth, crack inclination angle, angle between induction currents and the crack and the materials influence were investigated systematically. It was found, that for small cracks the signal first depends linearly both on crack length and crack depth and reaches a saturation for large crack dimensions. The signal decreases slowly, when the induction current no longer flowing perpendicular to the crack. But even for parallel incident flow the signal is still 25 to 30% of the maximum signal. For inclined cracks, the thermal signal first increases with deviation from the perpendicular and later decreases. This favours detection of typical surface defect types occurring in forging processes.

Cracks parallel to the surface can be detected by their interaction with the thermal pulse, when their lateral dimension is larger than their depth. If sub-surface perpendicular cracks are to be detected, the top of the crack has to be within half of the skin depth from the surface.

Crack type	Conditions	Crack length L	Crack detectable, if
Open perpendicular		L>=7.5 mm	depth>=0.15 mm
		2 mm <=L<7.5 mm	depth>=0.25 mm
Open inclined	20°<crack angle with surface < 60°	L>=7.5 mm	depth>=0.08 mm
		2 mm <=L<7.5 mm	depth>=0.15 mm
Covered	perpendicular	L>=7.5 mm	depth<=δ/2
	parallel	L: minimum lateral dimension	depth<=L

Table 2: Present detection limits in ferritic steel. δ is the electromagnetic skin depth

Table 2 shows achieved crack detection limits for ferritic materials using our present equipment for a signal-to-noise (background) ratio better than 6 dB.

The limiting factors are often the roughness of the technical surfaces and sometimes surface contaminations rather than the signal-to-noise of the thermal detector. Disturbing influences due to industrial dust, corrosion, oil films, scale and metal chips were investigated. It turns out, that most of these influences can be removed by simple measures or can be suppressed by signal processing. In contrast to visual or magnetic particle inspection is turns out to advantageous that additional information is available in the temporal dynamics of the thermographic image sequence.

5. Series Investigation

In a series investigation comprising 84 small complex-shaped forged components as shown in Fig. 7, the detection and false alarm rate of thermography was compared to that of conventional magnetic particle (MP) inspection. The components were taken from a seed of parts classified as defective after conventional MP testing, as routinely performed by the manufacturer in series production.

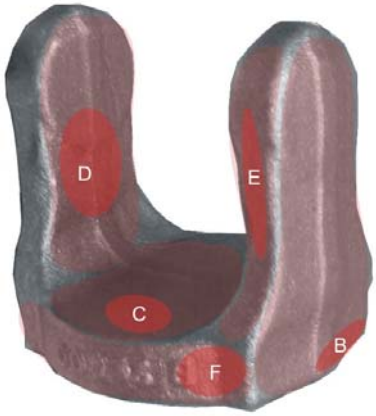

Fig. 7: Component with markings at typical defect positions

The components were all tested by induction thermography as described above, which resulted in 11 components with defect indications. Then, they were characterized by a more rigorous MP inspection in the laboratory and finally by metallography at the positions of defect indications. The evaluation shows, that the number of 37 components with defect indications from initial MP testing had to be reduced to 11 with verified serious defects. The defect indications from thermography were all verified. In two components with defect indications by MP testing, which were no detected by thermography, metallography revealed covered inclusions regarded as not critical by the manufacturer. Induction thermography turned out to show all relevant defects and to have a much smaller false alarm rate.

6. Automatization

Testing concepts for mass products are based on roboter handling of the test objects and induction coils, where they are inspected from different directions and on all relevant surfaces.

Induction currents are applied in different directions. As testing time for a single view is only 100 ms, two parts can be completely tested within 13 s.

7. Conclusion

Induction thermography allows fast and contact-free testing of ferritic steel components, even if they have a complex shape. A high probability of detection and a low false alarm rate were achieved. This together with the high testing speed and the absence of chemicals render induction thermography an interesting alternative to magnetic particle testing. In principle, volume defects close to the surface can be detected as well. By analysing the time dependence of the temperature signal, a course classification of defect depth is possible.

References

[1] K.-J. Kremer, 'Das THERM-O-MATIC-Verfahren - Ein neuartiges Verfahren für die Online-Prüfung von Stahlerzeugnissen auf Oberflächenfehler', in: "3rd European Conference in Nondestructive Testing", Florence 15- 18 October 1984, S. 171-186

[2] D. M. Heath and W. P. Winfree, Rev. Progr. Quant. Nondestr. Eval. **9**, D. O. Thompson and D. E. Chimenti (eds.), (Plenum Press New-York 1990), 577-584

[3] J. Bamberg, G. Erbeck, G. Zenzinger, 'Eddy-Therm: Ein Verfahren zur bildgebenden Prüfung metallischer Bauteile', ZfP-Zeitung **68** (1999) 60-62

[4] G. Riegert, T. Zweschper, G. Busse, 'Lockin thermography with eddy current excitation', QIRT Journal **1** (2004) 21-32

[5] B. Oswald-Tranta, 'Thermoinductive investigations of magnetic materials for surface cracks', QIRT Journal **1** (2004) 33-46

[6] G. Walle, U. Netzelmann, 'Thermographic Crack Detection in Ferritic Steel Components Using Inductive Heating', Proc. 9th ECNDT Berlin, 25.-29.9.2006, DGZfP Berichtsband BB 103-CD, Paper Tu.4.8.5

[7] J. Vrana, M. Goldammer, J. Baumann, M. Rothenfusser, W. Arnold: 'Mechanisms and Models for Crack Detection with Induction Thermography', Rev. QNDE **27** (2008), D.O. Thompson, D.E. Chimenti (eds), Melville: AIP (2008), to be published

[8] F. Wolf, 'Experimentelle Untersuchungen zum Einfluss der Fehlergeometrie auf das Nachweisvermögen der induktiven Thermografie bei unterschiedlichen Materialien', Batchelor thesis, HTW des Saarlandes and Fraunhofer IZFP, 2007

[9] H. Strauß, 'Untersuchungen zur Charakterisierung von Oberflächenrissen sowie verdeckten Rissen in ferromagnetischen Materialien mittels einer thermischen Prüftechnik mit induktiver Anregung', Diploma thesis, Universität des Saarlandes and Fraunhofer IZFP, 2007